**Investigating the Roles of Homeobox Proteins and TEAD in Small Cell Lung Cancer**

by

Bea Ricarte

A thesis submitted to the Department of Biological Sciences, University of Manitoba,

in partial fulfilment of the requirements for the course

BIOL 4100 (Honours Thesis)

for the degree of

Bachelor of Science (Honours)

**Abstract**

Lung cancer remains a significant global health concern, responsible for a substantial number of cancer-related deaths annually. Small cell lung cancer (SCLC), one of its subtypes, is particularly aggressive and resistant to treatment, leading to a poor prognosis for patients. Unfortunately, treatment options for SCLC remain limited and have not been advanced for decades. This highlights the urgent need for a deeper understanding of the molecular mechanisms underlying the pathogenesis of SCLC in order to identify novel therapeutic strategies for this disease. DNA-bind proteins, TEADs, play a crucial role in promoting SCLC survival. TEADs are best recognized for their role in interacting with transcriptional activators, YAP and TAZ, however, it was found that the function of TEADs in SCLC is completely independent of YAP and TAZ. Beyond this however, the mechanisms underlying the critical function of TEAD in SCLC is unknown. Preliminary data gathered by the Pearson lab identified the presence of homeobox proteins PROX1, NKX2-1 and NKX2-2 with the TEAD complex in SCLC, prompting the hypothesis that TEAD interacts with these proteins to silence TEAD target genes in SCLC, promoting the cancerous state. Using co-immunoprecipiation, the association of TEAD with PROX1 and NKX2-1 were confirmed. Additionally, CRISPR interference was used to knockdown PROX1, NKX2-1 and NKX2-2 in SCLC cells, to assess their role in TEAD-mediated gene regulation. This resulted in an increase in controlled cell regulation and differentiation genes, and a decrease in SCLC biomarkers, consistent with the hypothesis. However, contrasting the hypothesis, protein knockdowns showed a decrease of cell adhesion genes. Nevertheless, these findings bring light to a novel pathway in SCLC pathogenesis. Understanding the exact mechanisms behind these homeobox proteins and their interaction with TEADs could lead to the development of more effective treatment for SCLC.

**Acknowledgements**

Firstly, I would like to thank my family, specifically my sister and friends who have showed me great support and positivity throughout the process of my honours thesis. I would also like to thank Dr. Joel Pearson who was the best supervisor to me. Throughout my time in his lab, my passion for science grew in many ways, and I hope to be a great teacher and researcher like him one day. Thank you for being a great mentor and helping me be a better student! Lastly, I would like to thank all members of my lab and those at CancerCare Research Institute for being such a welcoming group and helping me throughout my honours project.

**Table of Contents**

**List of Tables**

**List of Figures**

# 1. Introduction

## 1.1 Small Cell Lung Cancer

Lung cancer is the largest contributor to cancer-related deaths globally with an estimate of 2.2 million cases reported worldwide in 2020 (Horie et al. 2016; Wang et al. 2023; Yu et al. 2023). It stands as the most prevalent cancer in males, with an estimated 1.4 million incident cases, and the third most common cancer among females, with 0.77 million incident cases reported in 2020 and rising (Wang et al. 2023). Disease subtypes are classified into non–small cell lung cancer, small cell lung cancer (SCLC), and carcinoid (Clinical Lung Cancer Genome Project (CLCGP) and Network Genomic Medicine (NGM) 2013). Out of the different lung cancer subtypes, SCLC is the most dangerous and accounts for 15% of all lung cancers, demonstrating distinct pathological, biological, and clinical differences from the other subtypes (George et al. 2015; Horie et al. 2016; Gazdar et al. 2017; Wang et al. 2023). While the lung epithelium is thought to comprise of various stem cell types that give rise to the diverse cell types in the lungs, SCLC is believed to originate from neuroendocrine cells (Park et al. 2011).

SCLC is an extremely aggressive and lethal disease, affecting approximately 250,000 patients every year on a global scale, and leading to approximately 200,000 deaths (Wang et al. 2023). It is common in individuals who smoke, with smokers making up to 95% of all SCLC cases, suggesting that smoking is a major risk factor in this type of cancer (George et al. 2015; Wang et al. 2023). SCLC is defined by its early metastasis, rapid growth, and therapeutic resistance, making it highly aggressive, deadly, and difficult to treat (Rudin et al. 2019). Additionally, most cases have poor diagnosis at advanced stages due to their early metastasis, leading SCLC to be tagged as a “recalcitrant cancer” (George et al. 2015; Gazdar et al. 2017; Rudin et al. 2019).

SCLC treatments consist of surgery and radiation and are only effective in a minority of patients in the early stages of the disease due to its fast and aggressive metastasis, while advanced cases are generally only given cytotoxic chemotherapy and often lead to death within a few months of recurrence (Rudin et al. 2019; Pozo et al. 2021; Wang et al. 2023). Unfortunately, there have been no significant advances for SCLC treatment in the past several decades (Gazdar et al. 2017). This slow progress of available molecularly targeted drugs for SCLC can be attributed to the limited understanding of its underlying biology, contrasting the great progress made in therapeutics for the other lung cancer subtypes (Niederst et al. 2015; Lee et al. 2017; Rudin et al. 2019). This shortcoming highlights the importance of studying the molecular mechanisms of this disease to produce more effective therapies.

## 1.2 Hippo Pathway

The Hippo pathway, along with its regulators, acts to control organ size and cell number by regulating cell proliferation and apoptosis (Wu et al. 2008; Horie et al. 2016; Cho et al. 2019; Zhou et al. 2019). Accordingly, the physiological functions and regulation of this pathway across organisms has been the focus of substantial research (Wang et al. 2018; Zheng and Pan 2019). Because of its crucial role in maintaining normal conditions of tissue size this pathway has been largely conserved throughout evolution (Wang et al. 2018; Zheng and Pan 2019). However, malfunctions in this pathway are linked to dysfunctional tissue growth and thus, are related to tumorigenesis and cancer development (Chen et al. 2010; Kaan et al. 2017; Zheng and Pan 2019; Zhou et al. 2019; Guo et al. 2022). The major transcriptional regulators of the Hippo pathway are the nuclear effectors YAP and TAZ, which are transcriptional coactivators that primarily facilitate the expression of genes related to cell growth and anti-apoptosis (Zanconato et al. 2015; Kaan et

al. 2017; Pearson et al. 2021; Wang et al. 2023). When the Hippo pathway is active, kinases phosphorylate YAP/TAZ, resulting in YAP and TAZ to be isolated in the cytoplasm, and unable to promote the transcription (Kaan et al. 2017). When the Hippo pathway is inactive, YAP and TAZ are able to enter the nucleus and bind with TEAD family transcription factors, forming a YAP/TAZ/TEAD complex that activates transcription (Vassilev et al. 2001; Liu-Chittenden et al. 2012; Horie et al. 2016; Kaan et al. 2017). TEADs have four homologous proteins, TEAD1-4, which play a role in transcription mediated by YAP in the Hippo pathway (Vassilev et al. 2001; Chen et al. 2010; Lamar et al. 2012; Pobbati et al. 2015). Data from the Pearson lab (and others) have identified TEAD4 to be the most influential paralogue in SCLC (Pearson, unpublished).

Because YAP often works as a growth promoter in the Hippo pathway, it is also an oncogenic protein in a variety of cancers, defining these as $YAP^{on}$ cancers (Chen et al. 2010; Pearson et al. 2021). By contrast, there is an absence of YAP in some cancers, such as SCLC, which exhibit a YAP deficiency and are categorized as $YAP^{off}$ cancers (Pearson et al. 2021). When YAP is ectopically expressed in $YAP^{off}$ cancers, it causes tumor suppression through the induction of YAP adhesion ($YAP^{ad}$) genes (Pearson et al. 2021). Investigation of $YAP^{on}$ and $YAP^{off}$ cancers revealed that Activator Protein-1 (AP1) promoter sites, upstream DNA sequences associated with cell division, are present with YAP/TEAD-bound enhancers in $YAP^{on}$ cancers, while $YAP^{off}$ cancers instead show an enrichment of binding sites for lineage-determining homeobox and basic-loop-helix transcription factors, suggesting that the TEAD interactome is different in $YAP^{on}$ and $YAP^{off}$ cancers (Pearson et al. 2021).

Additionally, unpublished results from the Pearson lab have identified a critical YAP-independent function for TEADs in SCLC. The specific mechanisms through which TEADS exert

their distinctive roles in SCLC remain unclear. However, uncovering these mechanisms could introduce innovative therapeutic avenues for treating SCLC. To delve deeper into the mechanisms governing TEAD function in SCLC, research conducted by the Pearson lab utilized a proteomic strategy to pin-point TEAD-associated proteins in SCLC, leading to the identification of three homeobox partner proteins: PROX1, NKX2-1, and NKX2-2 (Figure 1). These homeobox proteins are also known to play a role in epithelial lung biology, however their exact roles are unknown (Lawson et al. 2011; Pozo et al. 2021). Due to their possible interactions with TEAD, these proteins potentially can be targeted to develop novel therapies for SCLC. Accordingly, I tested the hypothesis that TEAD associates with the specific homeobox proteins PROX1, NKX2-1, and NKX2-2, and that these proteins play a role in cooperating with TEADS in SCLC.

| | $YAP^{on}$ NSCLC | $YAP^{off}$ SCLC |
|---|---|---|
| PROX1 | 0 | 6.0 |
| NKX2-2 | 0 | 3.1 |
| NKX2-1 | 0 | 5.7 |

Figure 1. Relative abundance (log 2 transformed peptide spectral counts) of PROX1, NKX2-1, and NKX2-2 in TEAD4 BioID-Mass spectrometry screen within $YAP^{on}$ non-small cell lung cancer (NSCLC), and $YAP^{off}$ small cell lung cancer (SCLC) samples (Pearson, unpublished). The results reveal that PROX1, NKX2-1, and NKX2-2 are absent in non-small cell lung cancer cells and are present in small cell lung cancer cells.

## 2. Research Objectives

It is hypothesized that the cancerous state in $YAP^{off}$ cancers is maintained through the interaction of TEAD with PROX1, NKX2-1, and NKX2-2, which allows them to regulate the expression of specific target genes that promote tumor growth (Pearson, personal communication). Therefore, the TEAD complex makes an attractive subject of study when it comes to the inner machinery of $YAP^{off}$ cancers like SCLC. In order to further examine the TEAD complex and deduce its ability to silence TEAD target genes in SCLC, I studied the different partner proteins of TEAD in $YAP^{off}$ SCLC cancer (PROX1, NKX2-1, and NKX2-2), as these differ from those in $YAP^{on}$ cancers (Pearson et al. 2021). The TEAD complex in $YAP^{on}$ cancers contains AP1 proteins, which promote the expression of proliferation genes (Pearson et al. 2021). This is different to TEAD complexes in $YAP^{off}$ cancers like SCLC, which interact with basic-loop-helix/homeobox proteins (Pearson et al. 2021). Thus, I predicted that targeting homeobox partner proteins of the TEAD complex in SCLC will influence TEAD target genes.

My first objective was to determine the association of the partner proteins PROX1, NKX2-1, and NKX2-2 with the TEAD complex. In order to do so, I used the techniques of co-immunoprecipitation (CoIP) and western blotting, as these are complementary to each other to isolate and validate the presence of proteins interacting in a sample (Lo Sardo 2023). Briefly I used immunoprecipitation (IP) and isolated the protein of interest (TEAD4) through the use of specific antibodies and washed away any unwanted material. I then western blotted the sample with antibodies specific to my partner proteins of interest (PROX1, NKX2-1 and NKX2-2) and visualized using an ECL imager (Mahmood and Yang 2012).

To address if these specific proteins regulate TEAD target genes, I conducted a separate experiment using quantitative PCR (qPCR). Briefly, I knocked down the homeobox proteins, PROX1, NKX2-1, and NKX2-2 in SCLC cells, and assessed the expression of TEAD target genes using a real-time qPCR machine, Quantstudio5 (Nolan et al. 2006; Pearson and Bremner 2021).

## 3. Materials and Methods

### 3.1 Cell Culture and Maintenance

The NHI-H209 SCLC (H209) cell line obtained from the American Type Culture Collection was used in all protocols of this project. Following the methods of Pearson and Bremner (2021), the cells were grown in RPMI 1640 L-glutamine media base with 7.5% heat inactivated fetal bovine serum and kept incubated at 37°C in a humidified atmosphere with 5% $CO_2$. After 3-4 days of incubation, the H209 cell quantity is expected to double. To maintain cell viability and optimal density, cell passaging to a 1:1 cell to media ratio was performed every 3-4 days. Three variations of H209 cell lines were used: stalk H209 cells used in the knockdown experiments, and two lentivirus modified lines – one with induced TEAD overexpression, and the other using an empty vector, labelled as the Empty H209 cell line (Pearson and Bremner 2021).

### 3.2 Immunoprecipitation

Both the negative isotype control immunoprecipitation and the TEAD4 immunoprecipitation samples consisted of two different cell lines: Empty (still containing endogenous TEAD4), and TEAD4 (overexpressing TEAD4), resulting in the preparation of four samples. The collected cells were then washed with phosphate-buffered saline and subjected to a

lysis buffer consisting of 0.1% NP40, protease/phosphatases inhibitor cocktail (Cat# 5872, Cell Signalling Tech), and phenylmethylsulfonyl fluoride, allowing access to cellular components. To remove possible interfering DNA, the samples were sonicated and incubated with 1.25 µL of turbonuclease at 4℃ for 15 minutes. A portion of the samples were isolated and reserved in a Laemmli sample buffer for future use as input lysate (Laemmli 1970). The remaining lysates were then incubated with Protein G beads, alongside a control primary antibody in the control immunoprecipitation samples and the TEAD4 primary antibody in the TEAD4 immunoprecipitation samples (Normal Mouse IgG and TEF-3 Mouse Monoconal IgG respectively, Santa Cruz Biotechnology), for 3 hours at 4 ℃, in which the Protein G beads and the primary antibodies bind (Lo Sardo 2023). Following the incubation period, the samples underwent three washes with 1mL lysis buffer per wash. The final isolated protein products were then kept in Laemmeli sample buffer and stored at -80℃ (Laemmli 1970).

3.3 Viral Transduction

Lentivirus (prepared by Dr. Pearson) acts as a vector to introduce CRISPR interference (CRISPRi) components into the H209 cells, facilitating the knockdown of the proteins of interest. Specifically, the vector consists of CRISPRi components, a puromycin resistance gene, Cas9-KRAB fusion, and varying guide RNAs that target PROX1, NKX2-1, and NKX2-2 (Alerasool et al. 2020).

Stock H209 cells were collected and washed with phosphate-buffered saline. They were then counted and adjusted to 1 million cells per well in a 6-well plate. Subsequently, polybrene was introduced to each well at a concentration of 5 µg/mL to enhance the efficiency of the viral transduction. Approximately 700 – 800µL of the lentivirus was then added to the designated well

and incubated with the H209 cells overnight in a humidified atmosphere with 5% $CO_2$ at 37°C. Over the following two weeks, the cells were maintained every 3-4 days, in which puromycin was added at 1 μg/mL to select for successfully transduced cells. Following the 2-week incubation period, the cells were collected and washed with phosphate-buffered saline and divided into two groups for subsequent knockdown confirmation through western blotting, or RNA isolation and reverse transcription for qPCR analysis of TEAD target genes (Pearson and Bremner 2021).

### 3.4 Cell Lysis

After collection of the protein knockdown samples, cells were subjected to lysis buffer compromising of radioimmunoprecipitation assay buffer (Santa Cruz Biotech), protease/phosphatases inhibitor cocktail (Cat# 5872, Cell Signalling Tech), and phenylmethylsulfonyl to facilitate access to cellular protein content. Subsequently, a bicinchoninic acid (BCA) assay was conducted using a BCA assay kit as per the manufacturer's instructions (Pierce BCA Protein Assay Kit, Thermo Fisher Scientific) to determine the protein concentrations of each sample using a spectrophotometer. Based on these concentrations, 50μg of each sample was used for the western blot, which was then diluted using Laemmli sample buffer (Laemmli 1970).

### 3.5 Western Blot

To test for the presence of PROX1, NKX2-1, and NKX2-2 in the co-immunoprecipitation samples, as well as their absence in the CRISPRi samples, the same western blot conditions were applied to both samples (Mahmood and Yang 2012; Pearson and Bremner 2021; Cañada-García and Arévalo 2023). Briefly, the samples underwent heat treatment at 95°C for 5 minutes to allow for proper denaturation and were subsequently loaded onto 10% polyacrylamide gels. The gel

electrophoresis proceeded for >1 hour with conditions of 35mA per gel and 200V, in which the proteins in the sample were separated by their size. Following gel electrophoresis, the proteins of the gel were transferred to nitrocellulose membranes using the BioRad TransBlot Turbo Transfer System as per manufacturer's conditions, which were then blocked using a Tween 20 (TBST) and 5% milk solution for 1-2 hours. After the membranes underwent three 10-min washes with TBST, the membranes were subjected to an overnight incubation at 4°C with primary antibodies against PROX1, NKX2-1, and NKX2-2. After the primary antibody incubation, the membranes were washed three times with TBST for 10 min each and subjected to a secondary antibody incubation containing the horseradish peroxidase enzyme at room temperature for an hour, followed by another three washes with TBST. Chemiluminescence was then conducted by introducing an enhanced chemiluminescence compound (SuperSignal West Pico PLUS Chemiluminescent Substrate, Thermo Fisher Scientific), which oxidizes in the presence of the horseradish peroxidase enzyme, producing light for visualization. The membranes were then visualized using an ECL imager to assess the presence of PROX1, NKX2-1, and NKX2-2 in the co-immunoprecipitation samples, as well as confirm their absence in the CRISPRi knockdown samples. Additionally, CRISPRi knockdown western blots underwent semi-quantification using ImageJ.

3.6 Real-Time qPCR

The Monarch Total RNA Miniprep Kit (New England Biolabs) was then utilized to isolate RNA from the knockdown sample through specific filtered columns as per the manufacturer's instructions. The RNA isolations were then converted to complementary DNA (cDNA) through reverse transcription, using Invitrogen SuperScript IV VILLO Master Mix (Thermo Fisher Scientific) following the manufacturer's instructions. cDNA and primers corresponding to the

target genes of interest were incorporated with PowerTrack SYBR Green Master Mix (Thermo Fisher Scientific), which contains all the necessary components for qPCR amplification, such as a buffer solution, nucleotides, Taq polymerase, and a fluorescent dye for detection. The specific primer sequences for the target genes are detailed in Table 1. The mix underwent various temperature cycles in a thermocycler machine. The specific conditions consisted of an initial cycle of 95℃ for 2 min, followed by 40 cycles at 95℃ for 10 sec and 60℃ for 30 sec. The final cycle stage involved a temperature of 95℃ for 15 sec, 60℃ for 1 min, and 95℃ for 15 sec (Nolan et al. 2006). During this process, the target genes of interest are selectively amplified and quantified. Through this real-time qPCR process, a cycle threshold value for each target gene was determined using Design and Analysis 2.6.0 software (Thermo Fisher Scientific), which permits their relative expression to be calculated through the delta-delta cycle threshold method, with glyceraldehyde-3-phosphate dehydrogenase (GAPDH) and beta-actin (B-Actin) serving as housekeeping genes (Sikand et al. 2012).

| **Gene Card** (Stelzer et al. 2016) | **Forward Primer (5'-3')** | **Reverse Primer (5'-3')** | **Function** |
|---|---|---|---|
| NEUROD4 (Neuronal Differentiation 4) | ACTTGGCTTCTCTGACTGTC | TCCAGGATGGTGTGTTGAC | Involved in neuroendocrine differentiation (Vasiljevic et al. 2013). |
| HES1 (Hes Family BHLH Transcription Factor 1) | AACCAAAGACAGCATCTGAGCA | TCTTCAGAGCATCCAAAATCAGTGT | Associated with induced differentiation and arrested cell growth (Castella et al. 2000) |
| CHGA (Chromogranin A) | ATCGCTGAGGTCATCTCCGA | TGATGTCTCAGAATGGAAAGGAT | Biomarker for SCLC (Moss et al. 2009). |
| LATS2 (Large Tumor Suppressor Kinase 2) | CAGCAAGATGGGCTACCT | TGGTGGTAGGACGCAAAG | Suppression of lung cancer growth and migration (Yeung et al. 2016). |
| NKX2-2 (NK2 Homeobox 2) | AGAGCCTGCCCGTGAAG | ATCCAGACCGTGCAGGGA | Regulation of neuroendocrine cell fate lineages (Mio et al. 2023). |
| ZFP36L1 (ZFP36 Ring Finger Protein Like 1) | TCGTGTCTGCCACCATCTT | CAGTGCCTTTCTGTCCAG | Associated with cell proliferation and cell cycle progression (Enokido et al. 2024). |
| SULT1E1 (Sulfotransferase Family 1E Member 1) | TGCCACCTGAACTTCTTCCT | TGGACGACCAGCCACCATTA | Associated with apoptosis and suppressed cell growth (Xu et al. 2012) |
| GAPDH (Glyceraldehyde-3-Phosphate Dehydrogenase) | GACAGTCAGCCGCATCTTCT | TTAAAAGCAGCCCTGGTGAC | qPCR normalization (Sikand et al. 2012). |
| B-Actin (Actin Beta) | TCTTCCAGCCTTCCTTCCT | CAGCACTGTGTTGGCGTA | qPCR normalization (Sikand et al. 2012). |
| RGS4 (Regulator Of G Protein Signaling 4) | AAAGGGCTTGCAGGTCTG | CTTGTTGTGGGAAGAATTGTGT | GPCR regulator and reduces cell proliferation and migration (Aguilar et al. 2012). |
| CHGB (Chromogranin B) | CCAGTGGATAACAGGAACCA | TTCAGGACTTGGCGGCACT | Biomarker for SCLC (Moss et al. 2009). |
| KCNJ6 (Potassium Inwardly Rectifying Channel Subfamily J Member 6) | GCCAAGCTGACAGAATCCA | TGATGTGTCTTGGCAGGTCA | Detected in SCLC (Plummer et al. 2005). |
| NEURL1 | CATCACCTTCAGCAACCG | GGTCCTTGCTGGTGAAGC | Regulator in the Notch pathway (Teider et al. 2010). |

| | | | |
|---|---|---|---|
| (Neuralized E3 Ubiquitin Protein Ligase 1) | | | |
| PTPN14 (Protein Tyrosine Phosphatase Non-Receptor Type 14) | ATGTTCTATGTGC CAAATGTGTCA | TAGCCGAATCACC TGGTC | Phosphatase involved in cell adhesion and known tumor suppressor (Han et al. 2019). |

Table 1. Primer sequences and function of TEAD target genes and SCLC biomarkers used for qPCR analysis.

3.7 Statistical Methods

Three independent trials of qPCR were conducted with each trial quantifying the relative expression of TEAD target genes using the Design and Analysis 2.6.0 Software. The gene expression levels of TEAD target genes obtained from the three trials were averaged to provide a representative measure. Error bars were calculating using the standard deviation derived from the three trials to provide insight on the variability of the data. A one-tailed paired t-test was used to determine the statistical significance of the results. Specifically, significance was determined by comparing p-values obtained from the t-test to a significance level of 0.05. A p-value less than 0.05 was considered indicative of a statistically significant result.

## 4. Results

### 4.1 Testing the Association of TEAD with PROX1, NKX2-1, and NKX2-2

To assess the association of TEAD and homeobox proteins, I used H209 SCLC lines that either expressed an empty vector or overexpressed TEAD4. I conducted both a negative control and TEAD4 immunoprecipitation on these cell lines, in which an isotype control antibody and TEAD4 antibody, respectively, were used. The isotype control lanes (lanes 1 and 2, Figure 2) revealed no discernable bands, indicating the absence of nonspecific interactions. This control baseline served to confirm the specificity of the TEAD4 antibody. In contrast, the TEAD4 immunoprecipitation lanes (lanes 3 and 4, Figure 2) show specific banding with PROX1 and NKX2-1, and less pronounced banding in NKX2-2, which may be due to the non-specificity of the NKX2-2 antibody used. This observation firmly supports the hypothesis that these proteins are indeed associated with the TEAD complex in SCLC. Additionally, in the immunoprecipitation of TEAD4 from TEAD4 overexpressed cells (lane 4, Figure 2), I observed a higher level of co-precipitation with PROX1, and NKX2-1 compared to cells expressing only endogenous TEAD4 (lane 3). This finding further verifies the specificity of these interactions.

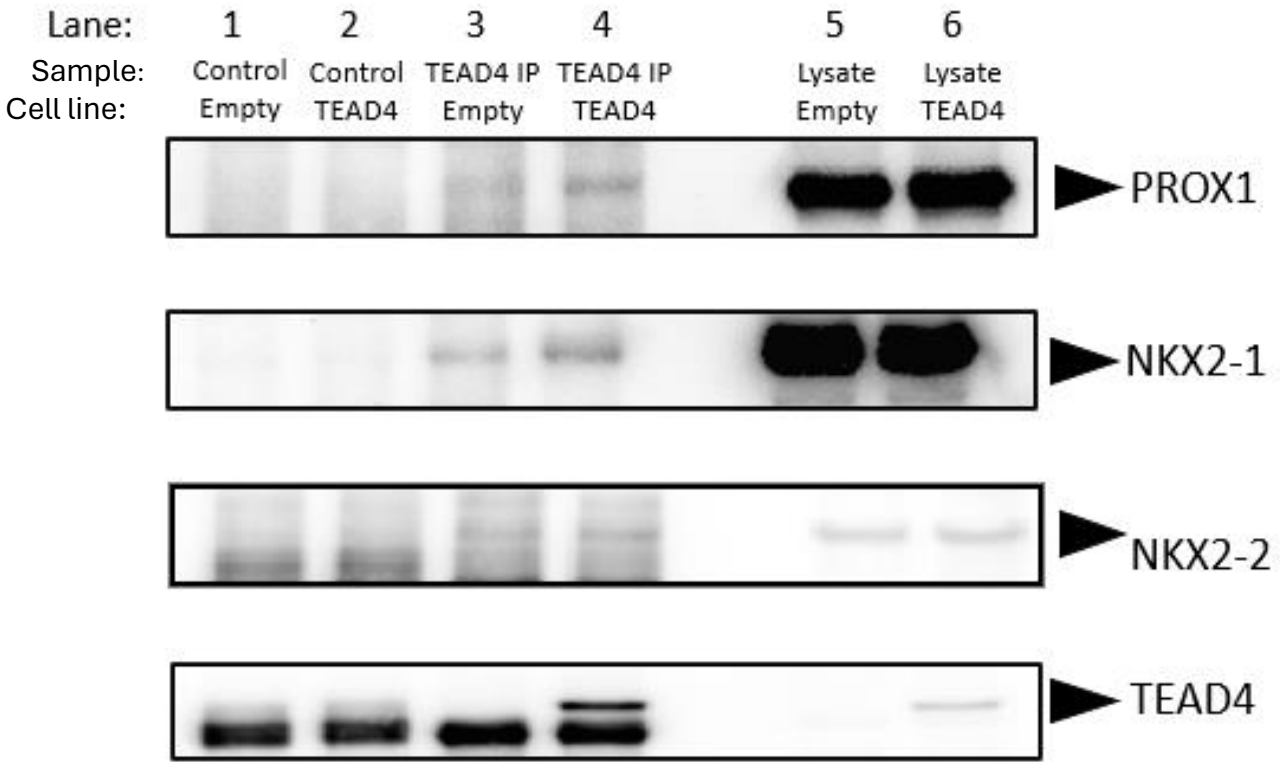


Figure 2. Western blot image demonstrating co-immunoprecipitation results targeting the TEAD complex in H209 cells. Control immunoprecipitation (IP) lanes (lanes 1 and 2, control empty cells and control TEAD4 overexpressed cells, respectively) show no specific bands confirming specificity. TEAD4 IP lanes (lanes 3 and 4) reveal distinct banding for PROX1, and NKX2-1 in association with TEAD4. NKX2-2 association is less clear. Lysates from empty and TEAD4 overexpressed cells (lanes 5 and 6) confirms its immunoprecipitation in the appropriate samples.

4.2 Confirming the Knockdown of PROX1, NKX2-1, and NKX2-2

To investigate the regulatory role of PROX1, NKX2-1 and NKX2-2, I used CRISPRi to down regulate each gene individually in H209 SCLC cells, with two distinct single guide RNAs (sgRNAs) for targeting each gene. Western blots and ImageJ were used to assess the impacts of knockdown of the three proteins on genes postulated to be regulated by TEAD4 (Figure 3 and 4). In comparison to the control cells in Figure 3 (1.0 quantification value), both PROX1 sgRNAs showed a clear decrease with PROX1 sgRNA #1 (lane 2) exhibiting almost complete knockdown (0.1 quantification value), while PROX1 sgRNA #2 (lane 3) exhibited around 60% knockdown (0.4 quantification value). Similarly, both NKX2-1 sgRNA (lanes 4 and 5) demonstrated moderate knockdown with NKX2-1 sgRNA #2 (lane 5) showing more efficient knockdown. Due to the inconsistencies experienced with the NKX2-2 antibody used, qPCR of the NKX2-2 gene was also conducted to provide insights into NKX2-2 knockdown at the RNA level (Figure. 5) alongside western blot confirmation (Figure. 4). Figure 4 quantification of NKX2-2 content demonstrates more efficient knockdown using sgRNAs #1 and #2 (lanes 2 and 3), which were used for the rest of the project. Figure 5 shows ~50% knockdown of NKX2-2 at the RNA level, with statistical significance only achieved in NKX2-2 sgRNA #2.

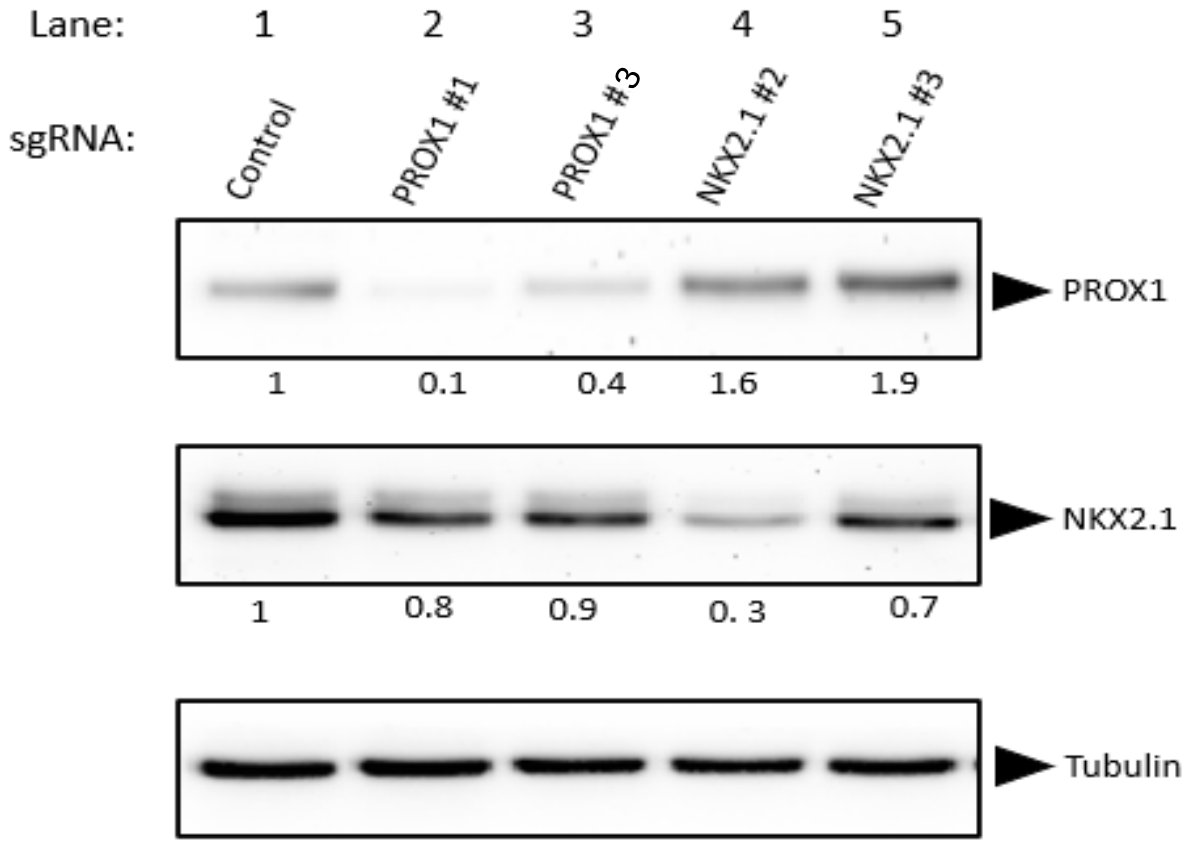


Figure 3. Western blot knockdown efficiency of PROX1 and NKX2-1 using lentiviral CRISPRi. Two different single guide RNAs (sgRNAs) were used for each protein target. Tubulin banding confirms similar loading between the samples. Numbers below experimental samples (control and knockdowns) represent semi-quantification of protein content.

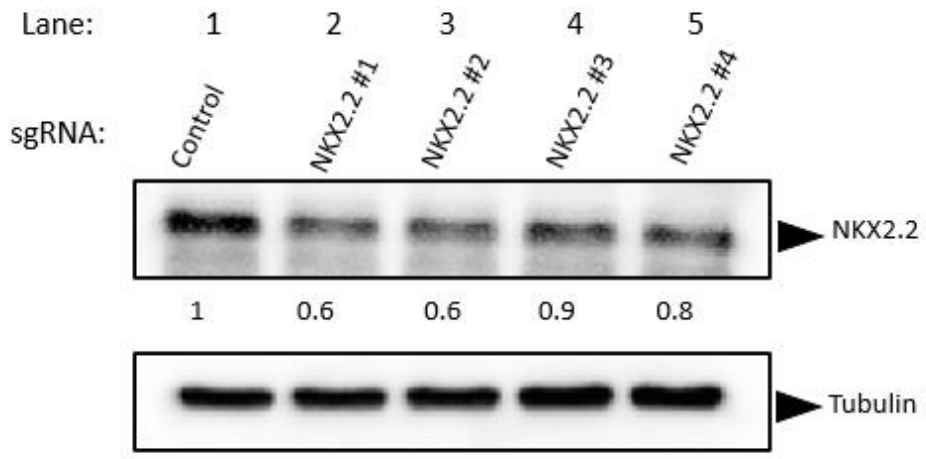


Figure 4. Western blot knockdown efficiency of NKX2-2 using lentiviral CRISPRi. Four different single guide RNAs (sgRNAs) were initially used to target NKX2-2. Tubulin banding confirms similar loading between the samples. Numbers below experimental samples (control and knockdowns) represent semi-quantification of protein content.

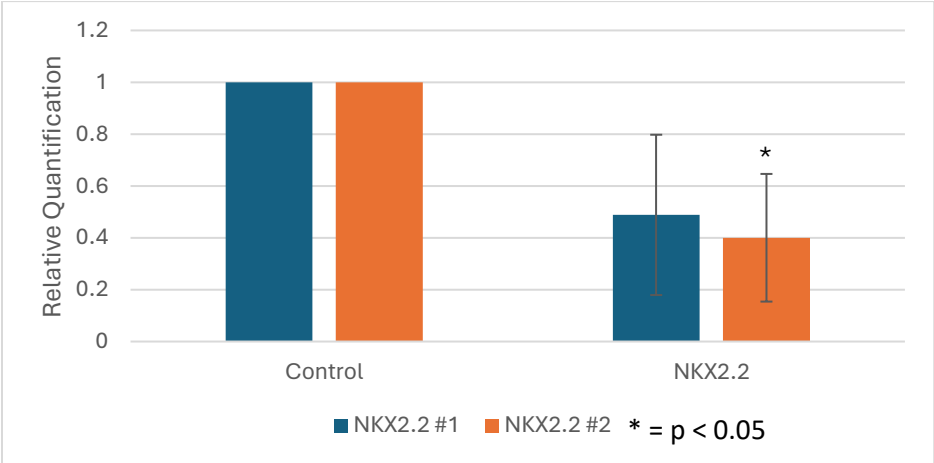


Figure 5. qPCR analysis of NKX2-2 RNA levels after CRISPRi knockdown using sgRNAs #1 and #2 (n=3).

4.3 Expression of TEAD Target Genes

HES1 expression levels exhibited a consistent increase using both PROX1 sgRNAs and NKX2-2 sgRNA #2 (Figure 6). Specifically, statistically significant increases were observed using PROX1 sgRNAs #1, and NKX2-2 #2, with knockdowns targeting PROX1 demonstrating the highest expression of HES1. Although NKX2-2 sgRNA #1 did not reach statistical significance, there was an upward trend of HES1 expression levels among the NKX2-2 knockdowns. However, knockdown of NKX2-1 did not lead to significant changes in HES1 expression (Figure 6). NKX2-2 knockdowns with sgRNA #2 resulted in a significantly decreased expression of LATS2, contrasting the prediction of increase following knockdown. Additionally, there were no significant changes to LATS2 expression with the other knockdowns. PTPN14 and ZFP36L expression decreased with the NKX2-1 knockdown using sgRNA #3 with statistical significance (differing from the prediction of increased expression) though demonstrating no significant changes in expression using the remaining knockdowns. Lastly, there were no significant changes observed in the expression of genes SULT1E1 and RGS4 following the knockdowns of PROX1, NKX2-1 and NKX2-2 (Figure 6).

A significant decrease in CHGA expression with NKX2-2 sgRNA #2 was observed (Figure 7). Although NKX2-2 sgRNA #1 did not reach statistical significance, a downward trend in CHGA expression was observed. However, knockdowns of PROX1 and NKX2-1 did not yield statistically significant changes. Similar to CHGA, knockdown of NKX2-2 with both sgRNAs resulted in a decrease of CHGB expression with statistically significance. However, PROX1 and NKX2-1 knockdowns did not result in statistically significant change in CHBG expression. Lastly, there

were no discernable change in gene expression of KCNJ6, NEURL1, and NEUROD4 following the knockdowns of PROX1, NKX2-1 and NKX2-2 (Figure 7).

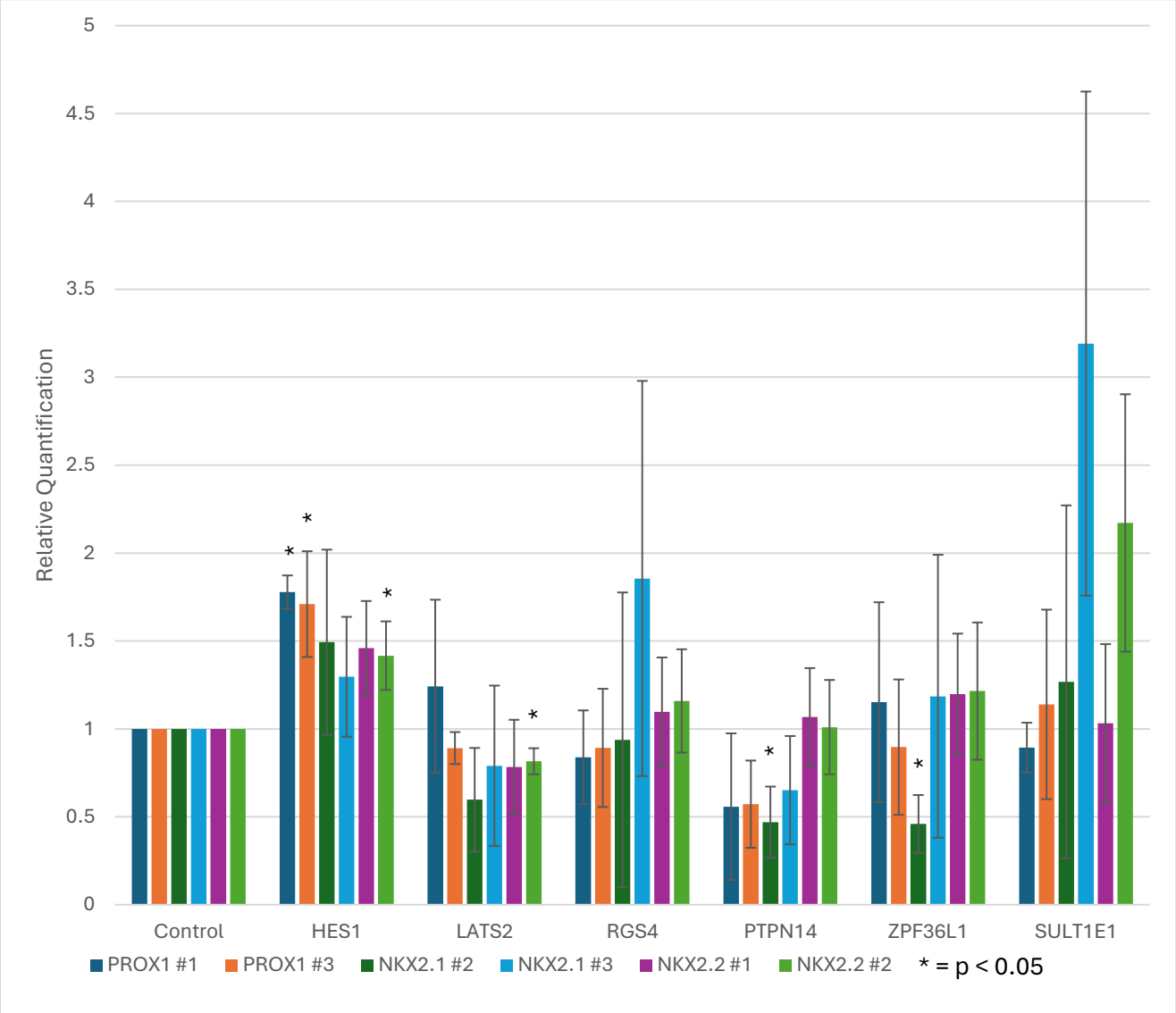


Figure 6. Real-time qPCR results displaying variation in TEAD target gene expression expected to increase following lentiviral CRISPRi knockdown of PROX1, NKX2-1, and NKX2-2 with varying guide RNAs incorporated. Relative gene expression was measured across 3 experimental trials (n=3). Asterisks denote statistical significance ($p < 0.05$) relative to control expression levels.

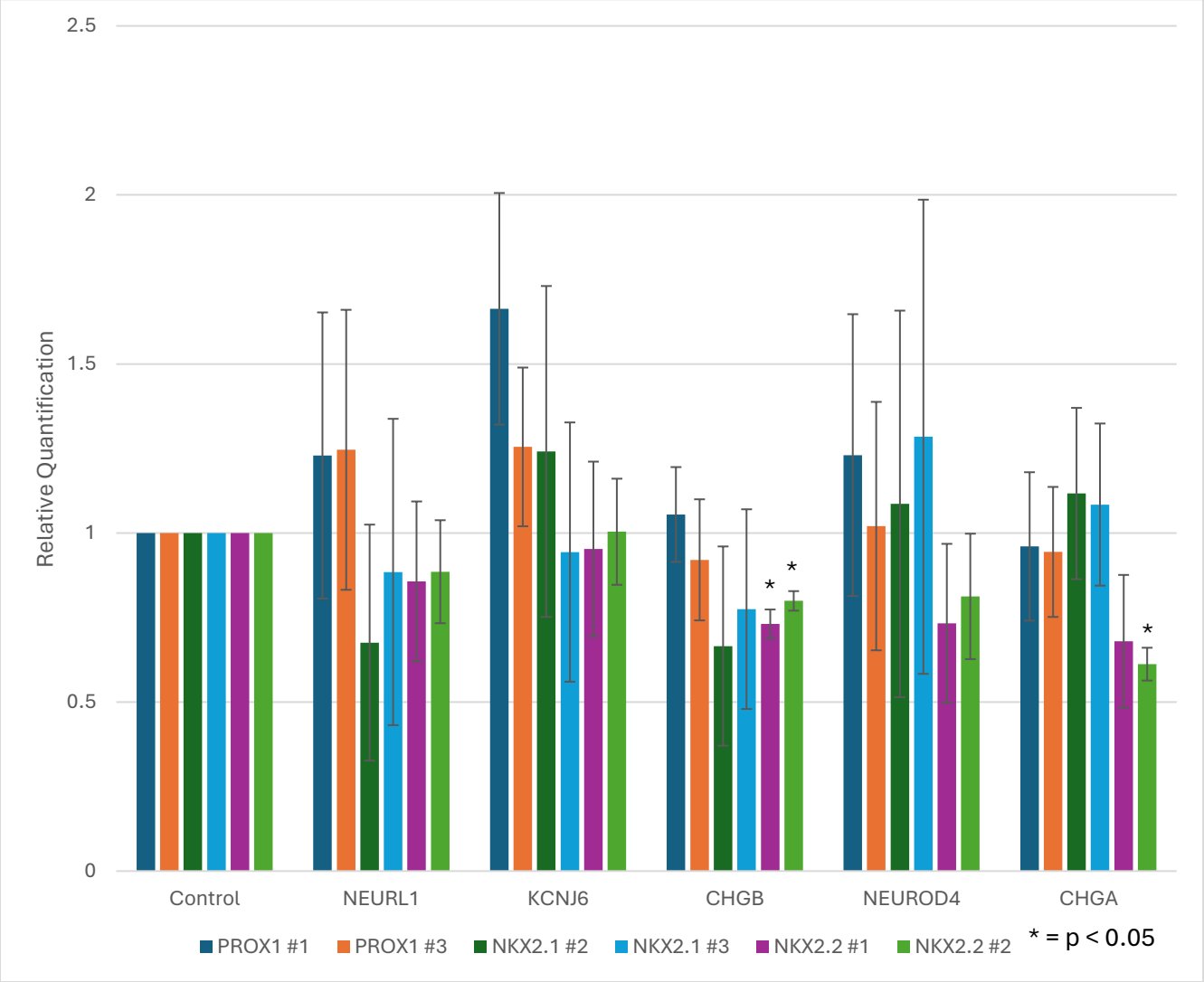


Figure 7. Real-time qPCR results showing variation in TEAD target gene expression expected to decrease after lentiviral CRISPRi knockdown of PROX1, NKX2-1, and NKX2-2 with varying guide RNAs incorporated. Relative gene expression was measured across 3 experimental trials (n= 3). Asterisks denote statistical significance ($p < 0.05$) relative to control expression levels.

## 5. Discussion

### 5.1 Association of PROX1, NKX2-1, and NKX2-2 with TEAD

The results from the co-immunoprecipitation confirm the association between PROX1 and NKX2-1 with the TEAD complex in H209 cells (Figure 2). The evident banding observed in the TEAD4 IP (lanes 3 and 4) — with the TEAD4 overexpressing cells exhibiting the most evident banding, as well as the absence of bands in the control IP lanes (lanes 1-2) — strongly support the specificity of these interactions in the context of SCLC. Additionally, the elevated levels of PROX1 and NKX2-1 in the lysates (lanes 5-6) suggest possible interactions outside of TEAD in SCLC. This is supported by previous literature demonstrating that both PROX1 and NKX2-1 interact with ASCL1 in SCLC to co-regulate genes in the NOTCH signalling pathway (Pozo et al. 2021). However, the interactions of NKX2-2 with the TEAD complex remains somewhat unclear, warranting further investigation through alternative techniques. Factors such as the specificity of the NKX2-2 antibody used may have contributed to this ambiguity. The lack of specificity of the NKX2-2 primary antibody was observed in both knockdown confirmation western blots as well as the co-immunoprecipitation western blots, indicating its overall ineffectiveness.

### 5.2 Modulation of TEAD Target Genes

Knockdown of PROX1 generally resulted in a statistically significant increase of HES1 expression using PROX1 sgRNA #1 and #3 (Figure 6), with the highest increase of HES1 expression found using the PROX1 sgRNA #1. This likely stems from the superior efficacy of the PROX1 sgRNA #1 in knocking down PROX1, which was confirmed by western blot analysis (Figure 3). The elevated expression of HES1 following PROX1 knockdown suggests a potential strategy to mitigate of SCLC severity, given HES1's involvement in induced cellular differentiation

and restrained cell growth (Castella et al. 2000). Specifically, given that HES1 serves as a downstream effector of the NOTCH pathway and considering its role in promoting cell differentiation that is distinct from the typical neuroendocrine pathway observed in this cancer, it is possible that elevated expression of HES1 is associated with the facilitation of cell maturation into non-neuroendocrine phenotypes (Tendler et al. 2020). As SCLC originates from neuroendocrine cells, maturation away from a neuroendocrine cell phenotype suggests a shift away from the typical characteristics associated with SCLC (Park et al. 2011).

Knockdown of NXK2-1 sgRNA #2 resulted in a significantly decreased expression of PTPN14 and ZFP36L1 (Figure 6). PTPN14 is a key phosphatase of the Hippo pathway involved in cell adhesion activity, while ZFP36L1 is associated with tumor suppression, and are therefore thought to play a role in inhibiting SCLC metastasis (Han et al. 2019; Tang et al. 2022; Enokido et al. 2024). The high potential of NKX2-1 to interact with other transcription factors or co-regulator proteins, as indicated by the input lysate lanes (lanes 5 and 6 of Figure 2), imply additional interactions beyond TEAD in SCLC regulation. Thus, it is possible that NKX2-1 interacts with other transcriptional regulators to influence the expression of PTPN14 and ZFP36L1, and the disruption of this unanticipated crosstalk could lead to changes in the regulation PTPN14 and ZFP36L1.

The NKX2-1 knockdown using sgRNA #3 resulted in the greatest variability across genes, suggesting off-target effects with this specific virus construct (Figure 6 and 7). This result aligns with the findings from the western blot analysis (Figure 3), which indicate a weaker knockdown efficiency for NKX2-1 sgRNA #3 (lane 5) compared to NKX2-1 sgRNA #2 (lane 4). Consequently, more instances of statistical significance are observed with NKX2-1 sgRNA #2. Furthermore,

another factor contributing to the absence or variability of effects on TEAD target gene expression could be gene redundancy. Given the known co-interactions between PROX1 and NKX2-1 in SCLC, it is plausible that the observed variability or limited effects result from the compensatory function of PROX1 when NKX2-1 is knocked down (Pozo et al. 2021).

Knockdown of NKX2-2 led to increased expression of HES1 which reached statistical significance with NKX2-2 sgRNA #2 (Figure 6). Although not achieving statistical significance with the NKX2-2 sgRNA #1, an upward trend of HES1 expression was observed following NKX2-2 knockdown. In contrast, LATS2 showed a statistically significant decrease following the knockdown induced by NKX2-2 sgRNA #2 which opposes the predicted increase. In non small cell lung cancer, LATS2 functions as a tumor suppressor, by inhibiting cell growth and migration through the phosphorylation of YAP, consequently hindering cell proliferation processes in non small cell lung cancer (Zhang et al. 2022). However, the absence of YAP in SCLC could suggest that LATS2 may exhibit responses different from the typical tumor suppressor role in non small cell lung cancer. Additionally, qPCR analysis (Figure 5) revealed a more effective downregulation of NKX2-2 using NKX2-2 sgRNA #2 (achieved statistical significance). This alongside consistent results in gene expression changes following NKX2-2 sgRNA #2 highlight the reliability of this construct.

A decrease in CHGB with both NKX2-2 sgRNAs was observed. CHBA is a neuroendocrine marker for SCLC, and this decrease in CHGB expression may impair neuroendocrine differentiation and disrupt neuroendocrine marker expression in SCLC cells, promoting a more noncancerous state (Yadav et al. 2023). CHGA also showed a general downward trend with NKX2-2 knockdown, although statistical significance is only achieved with NKX2-2

sgRNA #2. Similar to CHGB, CHGA is also a neuroendocrine marker and is a key characteristic of SCLC (Tlemsani et al. 2020). Thus, the down regulation of both these neuroendocrine biomarkers suggests lesser degree of SCLC state after NKX2-2 knockdown, highlighting their genetic regulatory roles in NKX2-2 in SCLC.

5.3 Limitations and Future Considerations

The potential for antibodies to function inadequately have likely introduced variability in the results, particularly evident in the case of NKX2-2. Consequently, the unreliability of the NKX2-2 antibody used was not sufficient to draw solid conclusions. To address this issue effectively, alternative techniques are required to accurately detect the association of NKX2-2 with TEAD as well as the success of protein knockdown through western blot. One alternative approach would be to involve genetically modified cell lines with NKX2-2 attached to an HA tag, also known as epitope tagging. The co-immunoprecipitation protocol can be repeated with using an HA primary antibody instead. Due to the consistency of the HA tag across many applications, this method is likely to enhance the reliability of the results and mitigate the issues with an uncertain antibody such as the NKX2-2 antibodies used (Zhao et al. 2019).

To address the potential gene redundancy between PROX1, NKX2-1 and NKX2-2 following protein knockdown, most likely to occur between PROX1 and NKX2-1, gene knockout experiments can be conducted to first confirm compensatory functions. This process involves deactivating one protein and assessing whether the other proteins can fulfill its functions in its absence, and vice versa (Ishibashi et al. 2020). Subsequently, double or multiple knockouts can be performed to completely mitigate the effects of redundancy behind suppressing gene expression (Chen et al. 2014). However, it is possible that knocking out essential proteins can have lethal

consequences and may result in unexpected results due to interactions with other proteins. For instance, considering the potential interactions of PROX1 and NKX2-1 beyond TEAD, as observed in the lysates (Figure 2), completely knocking out both proteins could possibly lead to unintended consequences in my samples. Alternatively, RNA interference (RNAi) can be utilized to reduce the expression of multiple genes simultaneously. This method is often considered more transient and less lethal compared to gene knockout approaches, providing a method to efficiently silence expression PROX1, NKX2-1, and NKX2-2, while minimizing the risk of adverse effects on cell viability and protein interactions (Agrawal et al. 2003).

In summary, the findings of this study contribute to our understanding of the intricate interplay between PROX1, NKX2-1 and NKX2-2 with the TEAD complex in SCLC. By confirming the association of PROX1 and NKX2-1 with TEAD in SCLC and emphasizing the regulatory functions of NKX2-2 in neuroendocrine differentiation, this research enhances our understanding of SCLC pathogenesis. Additionally, the identification of regulatory roles for PROX1 on genes such as HES1 provides critical insights into the molecular mechanisms driving SCLC. Moving forward, more research is required for addressing potential redundancy behind these transcription factors, as these discoveries may allow for investigations into the therapeutic potential of targeting these transcription factors, potentially introducing novel strategies for the management and treatment of SCLC.

## 6. Literature Cited


Agrawal, N., Dasaradhi, P.V.N., Mohmmed, A., Malhotra, P., Bhatnagar, R.K., and Mukherjee, S.K. 2003. RNA interference: biology, mechanism, and applications. Microbiol Mol Biol Rev **67**(4): 657–685. doi:10.1128/MMBR.67.4.657-685.2003.

Aguilar, B., Choi, I., Choi, D., Chung, H.K., Lee, S., Yoo, J., Lee, Y.S., Maeng, Y.S., Lee, H.N., Park, E., Kim, K.E., Kim, N.Y., Baik, J.M., Jung, J.U., Koh, C.J., and Hong, Y.-K. 2012. Lymphatic reprogramming by Kaposi sarcoma herpes virus promotes the oncogenic activity of the virus-encoded G-protein-coupled receptor. Cancer Res **72**(22): 5833–5842. doi:10.1158/0008-5472.CAN-12-1229.

Alerasool, N., Segal, D., Lee, H., and Taipale, M. 2020. An efficient KRAB domain for CRISPRi applications in human cells. Nat Methods **17**(11): 1093–1096. doi:10.1038/s41592-020-0966-x.

Cañada-García, D., and Arévalo, J.C. 2023. A simple, reproducible procedure for chemiluminescent western blot quantification. Bio Protoc **13**(9): e4667. doi:10.21769/BioProtoc.4667.

Castella, P., Sawai, S., Nakao, K., Wagner, J.A., and Caudy, M. 2000. HES-1 repression of differentiation and proliferation in PC12 cells: role for the helix 3-helix 4 domain in transcription repression. Mol Cell Biol **20**(16): 6170–6183. doi:10.1128/MCB.20.16.6170-6183.2000.

Chen, L., Chan, S.W., Zhang, X., Walsh, M., Lim, C.J., Hong, W., and Song, H. 2010. Structural basis of YAP recognition by TEAD4 in the Hippo pathway. Genes Dev **24**(3): 290–300. doi:10.1101/gad.1865310.

Chen, X., Xu, F., Zhu, C., Ji, J., Zhou, X., Feng, X., and Guang, S. 2014. Dual sgRNA-directed gene knockout using CRISPR/Cas9 technology in *Caenorhabditis elegans*. Sci Rep **4**(1): 7581. doi:10.1038/srep07581.

Cho, H., Kim, J., Ahn, J.H., Hong, Y.-K., Mäkinen, T., Lim, D.-S., and Koh, G.Y. 2019. YAP and TAZ negatively regulate Prox1 during developmental and pathologic Lymphangiogenesis. Circ Res **124**(2): 225–242. doi:10.1161/CIRCRESAHA.118.313707.

Clinical Lung Cancer Genome Project (CLCGP) and Network Genomic Medicine (NGM). 2013. A genomics-based classification of human lung tumors. Sci Transl Med **5**(209): 209ra153. doi:10.1126/scitranslmed.3006802.

Enokido, T., Horie, M., Yoshino, S., Suzuki, H.I., Matsuki, R., Brunnström, H., Micke, P., Nagase, T., Saito, A., and Miyashita, N. 2024. Distinct microRNA signature and suppression of ZFP36L1 define ASCL1-positive lung adenocarcinoma. Molecular Cancer Research **22**(1): 29–40. doi:10.1158/1541-7786.MCR-23-0229.

Gazdar, A.F., Bunn, P.A., and Minna, J.D. 2017. Small-cell lung cancer: what we know, what we need to know and the path forward. Nat Rev Cancer **17**(12): 765. doi:10.1038/nrc.2017.106.

George, J., Lim, J.S., Jang, S.J., Cun, Y., Ozretić, L., Kong, G., Leenders, F., Lu, X., Fernández-Cuesta, L., Bosco, G., Müller, C., Dahmen, I., Jahchan, N.S., Park, K.-S., Yang, D., Karnezis, A.N., Vaka, D., Torres, A., Wang, M.S., Korbel, J.O., Menon, R., Chun, S.-M., Kim, D., Wilkerson, M., Hayes, N., Engelmann, D., Pützer, B., Bos, M., Michels, S., Vlasic, I., Seidel, D., Pinther, B., Schaub, P., Becker, C., Altmüller, J., Yokota, J., Kohno, T., Iwakawa, R., Tsuta, K., Noguchi, M., Muley, T., Hoffmann, H., Schnabel, P.A.,

Petersen, I., Chen, Y., Soltermann, A., Tischler, V., Choi, C., Kim, Y.-H., Massion, P.P., Zou, Y., Jovanovic, D., Kontic, M., Wright, G.M., Russell, P.A., Solomon, B., Koch, I., Lindner, M., Muscarella, L.A., la Torre, A., Field, J.K., Jakopovic, M., Knezevic, J., Castaños-Vélez, E., Roz, L., Pastorino, U., Brustugun, O.-T., Lund-Iversen, M., Thunnissen, E., Köhler, J., Schuler, M., Botling, J., Sandelin, M., Sanchez-Cespedes, M., Salvesen, H.B., Achter, V., Lang, U., Bogus, M., Schneider, P.M., Zander, T., Ansén, S., Hallek, M., Wolf, J., Vingron, M., Yatabe, Y., Travis, W.D., Nürnberg, P., Reinhardt, C., Perner, S., Heukamp, L., Büttner, R., Haas, S.A., Brambilla, E., Peifer, M., Sage, J., and Thomas, R.K. 2015. Comprehensive genomic profiles of small cell lung cancer. Nature **524**(7563): 47–53. doi:10.1038/nature14664.

Guo, Y., Zhu, Z., Huang, Z., Cui, L., Yu, W., Hong, W., Zhou, Z., Du, P., and Liu, C.-Y. 2022. CK2-induced cooperation of HHEX with the YAP-TEAD4 complex promotes colorectal tumorigenesis. Nat Commun **13**(1): 4995. doi:10.1038/s41467-022-32674-6.

Han, X., Sun, T., Hong, J., Wei, R., Dong, Y., Huang, D., Chen, J., Ren, X., Zhou, H., Tian, W., and Jia, Y. 2019. Nonreceptor tyrosine phosphatase 14 promotes proliferation and migration through regulating phosphorylation of YAP of Hippo signaling pathway in gastric cancer cells. J Cell Biochem **120**(10): 17723–17730. doi:10.1002/jcb.29038.

Horie, M., Saito, A., Ohshima, M., Suzuki, H.I., and Nagase, T. 2016. YAP and TAZ modulate cell phenotype in a subset of small cell lung cancer. Cancer Sci **107**(12): 1755–1766. doi:10.1111/cas.13078.

Ishibashi, A., Saga, K., Hisatomi, Y., Li, Y., Kaneda, Y., and Nimura, K. 2020. A simple method using CRISPR-Cas9 to knock-out genes in murine cancerous cell lines. Sci Rep **10**(1): 22345. doi:10.1038/s41598-020-79303-0.

Kaan, H.Y.K., Chan, S.W., Tan, S.K.J., Guo, F., Lim, C.J., Hong, W., and Song, H. 2017. Crystal structure of TAZ-TEAD complex reveals a distinct interaction mode from that of YAP-TEAD complex. Sci Rep **7**(1): 2035. doi:10.1038/s41598-017-02219-9.

Laemmli, U.K. 1970. Cleavage of structural proteins during the assembly of the head of bacteriophage T4. Nature **227**(5259): 680–685. doi:10.1038/227680a0.

Lamar, J.M., Stern, P., Liu, H., Schindler, J.W., Jiang, Z.-G., and Hynes, R.O. 2012. The Hippo pathway target, YAP, promotes metastasis through its TEAD-interaction domain. Proc Natl Acad Sci U S A **109**(37): E2441-2450. doi:10.1073/pnas.1212021109.

Lawson, M.H., Cummings, N.M., Rassl, D.M., Russell, R., Brenton, J.D., Rintoul, R.C., and Murphy, G. 2011. Two novel determinants of etoposide resistance in small cell lung cancer. Cancer Res **71**(14): 4877–4887. doi:10.1158/0008-5472.CAN-11-0080.

Lee, J.-K., Lee, J., Kim, S., Kim, S., Youk, J., Park, S., An, Y., Keam, B., Kim, D.-W., Heo, D.S., Kim, Y.T., Kim, J.-S., Kim, S.H., Lee, J.S., Lee, S.-H., Park, K., Ku, J.-L., Jeon, Y.K., Chung, D.H., Park, P.J., Kim, J., Kim, T.M., and Ju, Y.S. 2017. Clonal history and genetic predictors of transformation into small-cell carcinomas from lung adenocarcinomas. J Clin Oncol **35**(26): 3065–3074. doi:10.1200/JCO.2016.71.9096.

Liu-Chittenden, Y., Huang, B., Shim, J.S., Chen, Q., Lee, S.-J., Anders, R.A., Liu, J.O., and Pan, D. 2012. Genetic and pharmacological disruption of the TEAD-YAP complex suppresses the oncogenic activity of YAP. Genes Dev **26**(12): 1300–1305. doi:10.1101/gad.192856.112.

Lo Sardo, F. 2023. Co-Immunoprecipitation (Co-Ip) in mammalian cells. Methods Mol Biol **2655**: 67–77. doi:10.1007/978-1-0716-3143-0_6.

Mahmood, T., and Yang, P.-C. 2012. Western blot: technique, theory, and trouble shooting. N Am J Med Sci **4**(9): 429–434. doi:10.4103/1947-2714.100998.

Mio, C., Baldan, F., and Damante, G. 2023. NK2 homeobox gene cluster: Functions and roles in human diseases. Genes Dis **10**(5): 2038–2048. doi:10.1016/j.gendis.2022.10.001.

Moss, A.C., Jacobson, G.M., Walker, L.E., Blake, N.W., Marshall, E., and Coulson, J.M. 2009. SCG3 transcript in peripheral blood is a prognostic biomarker for REST-deficient small cell lung cancer. Clinical Cancer Research **15**(1): 274–283. doi:10.1158/1078-0432.CCR-08-1163.

Niederst, M.J., Sequist, L.V., Poirier, J.T., Mermel, C.H., Lockerman, E.L., Garcia, A.R., Katayama, R., Costa, C., Ross, K.N., Moran, T., Howe, E., Fulton, L.E., Mulvey, H.E., Bernardo, L.A., Mohamoud, F., Miyoshi, N., VanderLaan, P.A., Costa, D.B., Jänne, P.A., Borger, D.R., Ramaswamy, S., Shioda, T., Iafrate, A.J., Getz, G., Rudin, C.M., Mino-Kenudson, M., and Engelman, J.A. 2015. RB loss in resistant EGFR mutant lung adenocarcinomas that transform to small-cell lung cancer. Nat Commun **6**: 6377. doi:10.1038/ncomms7377.

Nolan, T., Hands, R.E., and Bustin, S.A. 2006. Quantification of mRNA using real-time RT-PCR. Nat Protoc **1**(3): 1559–1582. doi:10.1038/nprot.2006.236.

Park, K.-S., Liang, M.-C., Raiser, D.M., Zamponi, R., Roach, R.R., Curtis, S.J., Walton, Z., Schaffer, B.E., Roake, C.M., Zmoos, A.-F., Kriegel, C., Wong, K.-K., Sage, J., and Kim, C.F. 2011. Characterization of the cell of origin for small cell lung cancer. Cell Cycle **10**(16): 2806–2815. doi:10.4161/cc.10.16.17012.

Pearson, J.D., and Bremner, R. 2021. Lentiviral-mediated ectopic expression of YAP and TAZ in YAPoff cancer cell lines. STAR Protoc **2**(4): 100870. doi:10.1016/j.xpro.2021.100870.

Pearson, J.D., Huang, K., Pacal, M., McCurdy, S.R., Lu, S., Aubry, A., Yu, T., Wadosky, K.M., Zhang, L., Wang, T., Gregorieff, A., Ahmad, M., Dimaras, H., Langille, E., Cole, S.P.C., Monnier, P.P., Lok, B.H., Tsao, M.-S., Akeno, N., Schramek, D., Wikenheiser-Brokamp, K.A., Knudsen, E.S., Witkiewicz, A.K., Wrana, J.L., Goodrich, D.W., and Bremner, R. 2021. Binary pan-cancer classes with distinct vulnerabilities defined by pro- or anti-cancer YAP/TEAD activity. Cancer Cell **39**(8): 1115-1134.e12. Elsevier. doi:10.1016/j.ccell.2021.06.016.

Plummer, H.K., Dhar, M.S., Cekanova, M., and Schuller, H.M. 2005. Expression of G-protein inwardly rectifying potassium channels (GIRKs) in lung cancer cell lines. BMC Cancer **5**: 104. doi:10.1186/1471-2407-5-104.

Pobbati, A.V., Han, X., Hung, A.W., Weiguang, S., Huda, N., Chen, G.-Y., Kang, C., Chia, C.S.B., Luo, X., Hong, W., and Poulsen, A. 2015. Targeting the central pocket in human transcription factor TEAD as a potential cancer therapeutic strategy. Structure **23**(11): 2076–2086. doi:10.1016/j.str.2015.09.009.

Pozo, K., Kollipara, R.K., Kelenis, D.P., Rodarte, K.E., Ullrich, M.S., Zhang, X., Minna, J.D., and Johnson, J.E. 2021. ASCL1, NKX2-1, and PROX1 co-regulate subtype-specific genes in small-cell lung cancer. iScience **24**(9): 102953. doi:10.1016/j.isci.2021.102953.

Rudin, C.M., Poirier, J.T., Byers, L.A., Dive, C., Dowlati, A., George, J., Heymach, J.V., Johnson, J.E., Lehman, J.M., MacPherson, D., Massion, P.P., Minna, J.D., Oliver, T.G., Quaranta, V., Sage, J., Thomas, R.K., Vakoc, C.R., and Gazdar, A.F. 2019. Molecular subtypes of small cell lung cancer: a synthesis of human and mouse model data. Nat Rev Cancer **19**(5): 289–297. doi:10.1038/s41568-019-0133-9.

Sikand, K., Singh, J., Ebron, J.S., and Shukla, G.C. 2012. Housekeeping gene selection advisory: glyceraldehyde-3-phosphate dehydrogenase (GAPDH) and β-actin are targets of miR-644a. PLoS One **7**(10): e47510. doi:10.1371/journal.pone.0047510.

Stelzer, G., Rosen, N., Plaschkes, I., Zimmerman, S., Twik, M., Fishilevich, S., Stein, T.I., Nudel, R., Lieder, I., Mazor, Y., Kaplan, S., Dahary, D., Warshawsky, D., Guan-Golan, Y., Kohn, A., Rappaport, N., Safran, M., and Lancet, D. 2016. The GeneCards Suite: From gene data mining to disease genome sequence analyses. Curr Protoc Bioinformatics **54**: 1.30.1-1.30.33. doi:10.1002/cpbi.5.

Tang, X., Qi, C., Zhou, H., and Liu, Y. 2022. Critical roles of PTPN family members regulated by non-coding RNAs in tumorigenesis and immunotherapy. Front. Oncol. **12**: 972906. doi:10.3389/fonc.2022.972906.

Teider, N., Scott, D.K., Neiss, A., Weeraratne, S.D., Amani, V.M., Wang, Y., Marquez, V.E., Cho, Y.-J., and Pomeroy, S.L. 2010. Neuralized1 causes apoptosis and downregulates Notch target genes in medulloblastoma. Neuro Oncol **12**(12): 1244–1256. doi:10.1093/neuonc/noq091.

Tendler, S., Kanter, L., Lewensohn, R., Ortiz-Villalón, C., Viktorsson, K., and De Petris, L. 2020. The prognostic implications of Notch1, Hes1, Ascl1, and DLL3 protein expression in SCLC patients receiving platinum-based chemotherapy. PLoS ONE **15**(10): e0240973. doi:10.1371/journal.pone.0240973.

Tlemsani, C., Pongor, L., Elloumi, F., Girard, L., Huffman, K.E., Roper, N., Varma, S., Luna, A., Rajapakse, V.N., Sebastian, R., Kohn, K.W., Krushkal, J., Aladjem, M.I., Teicher, B.A., Meltzer, P.S., Reinhold, W.C., Minna, J.D., Thomas, A., and Pommier, Y. 2020. SCLC-CellMiner: A resource for small cell lung cancer cell line genomics and pharmacology

based on genomic signatures. Cell Reports **33**(3): 108296. doi:10.1016/j.celrep.2020.108296.

Vasiljevic, A., Champier, J., Figarella-Branger, D., Wierinckx, A., Jouvet, A., and Fèvre-Montange, M. 2013. Molecular characterization of central neurocytomas: Potential markers for tumor typing and progression. Neuropathology **33**(2): 149–161. doi:10.1111/j.1440-1789.2012.01338.x.

Vassilev, A., Kaneko, K.J., Shu, H., Zhao, Y., and DePamphilis, M.L. 2001. TEAD/TEF transcription factors utilize the activation domain of YAP65, a Src/Yes-associated protein localized in the cytoplasm. Genes Dev **15**(10): 1229–1241. doi:10.1101/gad.888601.

Wang, Q., Gümüş, Z.H., Colarossi, C., Memeo, L., Wang, X., Kong, C.Y., and Boffetta, P. 2023. SCLC: Epidemiology, risk factors, genetic susceptibility, molecular pathology, screening, and early detection. J Thor Oncol **18**(1): 31–46. doi:10.1016/j.jtho.2022.10.002.

Wang, Y., Xu, X., Maglic, D., Dill, M.T., Mojumdar, K., Ng, P.K.-S., Jeong, K.J., Tsang, Y.H., Moreno, D., Bhavana, V.H., Peng, X., Ge, Z., Chen, H., Li, J., Chen, Z., Zhang, H., Han, L., Du, D., Creighton, C.J., Mills, G.B., Cancer Genome Atlas Research Network, Camargo, F., and Liang, H. 2018. Comprehensive molecular characterization of the hippo signaling pathway in cancer. Cell Rep **25**(5): 1304-1317.e5. doi:10.1016/j.celrep.2018.10.001.

Wu, S., Liu, Y., Zheng, Y., Dong, J., and Pan, D. 2008. The TEAD/TEF family protein Scalloped mediates transcriptional output of the Hippo growth-regulatory pathway. Dev Cell **14**(3): 388–398. doi:10.1016/j.devcel.2008.01.007.

Xu, Y., Liu, X., Guo, F., Ning, Y., Zhi, X., Wang, X., Chen, S., Yin, L., and Li, X. 2012. Effect of estrogen sulfation by SULT1E1 and PAPSS on the development of estrogen-dependent cancers. Cancer Sci **103**(6): 1000–1009. doi:10.1111/j.1349-7006.2012.02258.x.

Yadav, G.P., Wang, H., Ouwendijk, J., Cross, S., Wang, Q., Qin, F., Verkade, P., Zhu, M.X., and Jiang, Q.-X. 2023. Chromogranin B (CHGB) is dimorphic and responsible for dominant anion channels delivered to cell surface via regulated secretion. Front. Mol. Neurosci. **16**: 1205516. doi:10.3389/fnmol.2023.1205516.

Yeung, B., Yu, J., and Yang, X. 2016. Roles of the H ippo pathway in lung development and tumorigenesis. Intl Journal of Cancer **138**(3): 533–539. doi:10.1002/ijc.29457.

Yu, N., Hwang, M., Lee, Y., Song, B.R., Kang, E.H., Sim, H., Ahn, B.-C., Hwang, K.H., Kim, J., Hong, S., Kim, S., Park, C., and Han, J.-Y. 2023. Patient-derived cell-based pharmacogenomic assessment to unveil underlying resistance mechanisms and novel therapeutics for advanced lung cancer. J Exp Clin Cancer Res **42**(1): 37. doi:10.1186/s13046-023-02606-3.

Zanconato, F., Forcato, M., Battilana, G., Azzolin, L., Quaranta, E., Bodega, B., Rosato, A., Bicciato, S., Cordenonsi, M., and Piccolo, S. 2015. Genome-wide association between YAP/TAZ/TEAD and AP-1 at enhancers drives oncogenic growth. Nat Cell Biol **17**(9): 1218–1227. doi:10.1038/ncb3216.

Zhang, Y., Wang, Y., Ji, H., Ding, J., and Wang, K. 2022. The interplay between noncoding RNA and YAP/TAZ signaling in cancers: molecular functions and mechanisms. J Exp Clin Cancer Res **41**(1): 202. doi:10.1186/s13046-022-02403-4.

Zhao, N., Kamijo, K., Fox, P.D., Oda, H., Morisaki, T., Sato, Y., Kimura, H., and Stasevich, T.J. 2019. A genetically encoded probe for imaging nascent and mature HA-tagged proteins in vivo. Nat Commun **10**(1): 2947. doi:10.1038/s41467-019-10846-1.

Zheng, Y., and Pan, D. 2019. The Hippo signaling pathway in development and disease. Dev Cell **50**(3): 264–282. doi:10.1016/j.devcel.2019.06.003.

Zhou, W., Li, Y., Song, J., and Li, C. 2019. Fluorescence polarization assay for the identification and evaluation of inhibitors at YAP–TEAD protein–protein interface 3. Analytical Biochemistry **586**: 113413. doi:10.1016/j.ab.2019.113413.